Enhanced optical transmission by V-shaped nanoslit in metal film*

He Meng-Dong(贺梦冬)†, Ma Wang-Guo(马旺国), and Wang Xin-Jun(王新军)

Institute of Mathematics and Physics, Central South University of Forestry and Technology, Changsha 410004, *China*

(Received 21 November 2012; revised manuscript received 28 February 2013)

In this paper, we reveal that the enhanced transmission through a perforated metal film can be further boosted up by a V-shaped nanoslit, which consists of two connected oblique slits. The maximum transmission at resonance can be enhanced significantly by 71.5% in comparison with the corresponding vertical slit with the same exit width. The value and position of transmission resonance peak strongly depend on the apex angle of the V-shaped slit. The optimum apex angle, at which the transmission is maximal, is sensitive to the slit width. Such phenomena can be well explained by a concrete picture in which the incident wave drives free electrons on the slit walls. Moreover, we also simply analyze the splitting of the transmission peak in the symmetry broken V-shaped slit, originating from the resonances of different parts of the V-shaped slit. We expect that our findings will be used to design the nanoscale light sources based on the metal nanoslit structures.

Keywords: V-shaped nanoslit in metal film, enhanced optical transmission, surface plasmon polaritons

PACS: 42.25.Bs, 78.66.Bz, 73.20.Mf **DOI:** 10.1088/1674-1056/22/11/114201

1. Introduction

Enhanced transmission has become an important research direction in the emerging field of plasmonics since its discovery in 1998,[1] and such phenomena in several metal nanostructures ranging from periodic hole array to slit array have been deeply studied both theoretically[2–7] and experimentally.[8–14] Generally, it is admitted that the enhanced transmission can be understood as a resonance-wave-phenomenon related to the excitation of surface plasmon polariton (SPP) waves on both surfaces of metal film, and SPPs play an essential role through the physical process that the incident light is first converted to SPPs, then SPPs propagate along the slit/hole walls, before being converted back into light.[5] Interestingly, the transmission enhancement phenomenon also occurs in an isolated nanoslit[15,16] or a multi-slits metal structure,[17] the transmittance can exceed unity when it is normalized to the slit width. The reason is that a single nanoslit supports propagating modes as gap SPPs, which can lead to the single slit acting as a Fabry–Pérot (F–P) resonator.[16]

A single nanoslit is compact, amenable to integration, and it exhibits maximum transmission at the F–P resonance of guide mode with a length phase of an even integer of $\pi/2$, so a nanoslit is usually employed as a nanoscaled light source.[18,19] While the transmission through an isolated slit is too low for practical applications, a surprisingly large transmission can be obtained by adding auxiliary structures on the input surface of the slit, such as periodic/nonperiodic corrugations,[20–22] bumps,[23] a nanocavity antenna,[24] and a surface plasmon microcavity.[25] However, notice that there is difficulty in sample fabrication for these additional structures performed in the near-infrared and visible regimes. Furthermore, these additional structures significantly increase the slit size, which is not preferable for the high-density photonic circuit integration. From the research results in recent works,[26,27] we may obtain a method to solve the above shortcomings. It has been demonstrated that the transmission can be further enhanced by utilizing nanofocusing of radiation in tapered slits, since at the resonant wavelengths a larger entrance aperture could collect more light in comparison with a straight slit (whose channel is normal to the metal film surface).[26] The finding suggests that the transmission may be improved by changing the channel shape of the slit. Even though these works focus on the periodic slit structure, a similar conclusion can be obtained for a single tapered slit, since the considered transmission peak in the works is mainly originated from the F–P resonances of individual slits rather than the SPP excitation on both metal surfaces being coupled through the slit array. According to the view of charge-oscillation-induced light transmission,[28] in this paper, we propose a V-shaped slit structure, which consists of two connected oblique slits. We find that the enhanced transmission through a metal film can be further improved upon by the V-shaped nanoslit in comparison with that by the vertical slit. The transmission resonance peak is very sensitive to the apex angle of the V-shaped slit, and the optimum apex angle, at which the transmission is maximal, is influenced by the slit width. In addition, it is also found that the symmetry breaking of the V-shaped slit causes the splitting of the resonance peak. Our findings provide a new way to enhance the slit transmission and are helpful for designing a high-efficiency nanoscale light source based on composite metal nanoslit structures.

*Project supported by the National Natural Science Foundation of China (Grant No. 11174372) and the Youth Foundation of the Education Department of Hunan Province, China (Grant Nos. 11B134 and 10B118).

†Corresponding author. E-mail: hemendong@sohu.com

© 2013 Chinese Physical Society and IOP Publishing Ltd

2. Numerical model and simulations

Figure 1 depicts the two-dimensional schematic of a V-shaped nanoslit in a metal film being suspended in air, which is composed of two connected oblique slits with the same obliquity. A p-polarized (the magnetic field is perpendicular to the x–z plane) plane wave impinges normally on the top of the V-shaped slit. The V-shaped slit structure is characterized by the widths of left and right entrance W_1 and W_2 (the exit width W_1+W_2), the apex angle α, and the thickness of metal film H. The metal is chosen to be silver (Ag) and its dielectric function is referred to Ref. [29].

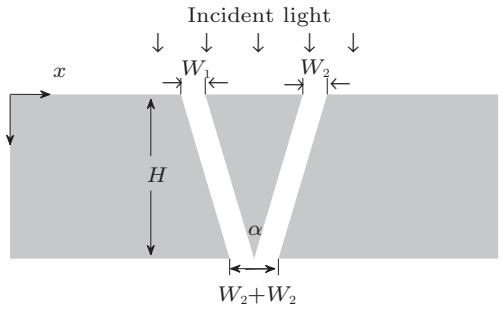


Fig. 1. Schematic configuration of a V-shaped nanoslit. A plane wave of TM polarization (the magnetic field is perpendicular to the x–z plane) is incident normally on the top of the structure.

We employ our two-dimensional finite-difference time-domain (2D-FDTD) program codes to simulate the interaction between the metal nanoslit and the incident wave. In the codes, the Maxwell's equations are discretized in space and time by central differences using Yee's cells,[30] and the current density is introduced into the Maxwell's equations due to the negative real part of permittivity of metal.[31] The simulation region is surrounded by a ten-cell-thick convolutional perfectly matched layer (i.e., CPML).[32] The spatial mesh cells are set to $\Delta x = \Delta z = \Delta s = 2.5$ nm, and the time step and the total number of time steps are taken as $\Delta t = \Delta s/2c$ (c is the velocity of light in vacuum) and 3×10^4, respectively. Such small size of cells and large total number of time steps ensure that the values of electromagnetic field and current density in spatial grids are convergent and stable. Since the size of cells is very small, the shape of channels of left/right oblique slit can be treated as a zigzag. Using the handling method, we calculated the transmission spectra of tapered slit structures in Refs. [26] and [27]. The simulated results are in good agreement with the theoretical and experimental results in these works, it confirms the validity of the above handling method. In this paper, we calculated the normalized transmission of the V-shaped slit, which is defined as $T_{\text{norm}} = [P_{\text{out}}/(W_1+W_2)]/(P_{\text{in}}/W_{\text{in}})$, where $P_{\text{in(out)}}$ is the power flux through in (out) the metal film, W_1+W_2 is the exit width of the V-shaped slit, and W_{in} is the lateral width of incident plane light.

3. Results and discussion

We start our discussion with the effect of apex angle α on the transmission spectrum. Figure 2(a) shows the normalized transmission spectra of the V-shaped slit structure at different values of α with fixed H and $W_1 = W_2$. In the special case of $\alpha = 0°$, the V-shaped slit is a single vertical slit with width $W = W_1 + W_2$, there is a resonance peak at about 640 nm, which is associated to the fundamental F–P resonance mode (with 2π phase length), and the resonance peak value is about 4.2. As α increases, the resonant peak exhibits a redshift and its amplitude is enhanced. Strictly speaking, the resonance peak stems from the interaction between the fundamental F–P resonance modes in the left and right oblique slits. At $\alpha = 90°$, the transmission peak is redshifted by 340 nm compared with that in the vertical slit. The transmission intensity reaches its maximum (about 7.2), and the transmission is improved by 71.5% in comparison with that in the vertical slit structure. Moreover, a new transmission peak appears in the short wavelength regime (at about 520 nm). Such peak is originated from the second order F–P resonance in the left/right oblique slit. With the further increase of α, both the long and short wavelength transmission peaks are redshifted and gradually drop. The red shifting of transmission resonance peak can be explained by the F–P resonance formula $\lambda_{\text{res}N} \simeq 2\text{Re}(n_{\text{eff}})L/N$ (where $\lambda_{\text{res}N}$ is the resonance wavelength of N-th order mode, $\text{Re}(n_{\text{eff}})$ is the real part of effective refractive index of slit, L is the slit length, and N is an integer).[33] Solving the transcendental equation of SPPs mode in the slit,[34] we may obtain n_{eff} of SPP mode. Figure 2(b) displays the dependence of $\text{Re}(n_{\text{eff}})$ on the effective width of oblique slit $[W_{1(2)}\cos(\alpha/2)]$ and the wavelength of SPP mode. From this figure, we know that, for a certain wavelength (effective width), $\text{Re}(n_{\text{eff}})$ increases

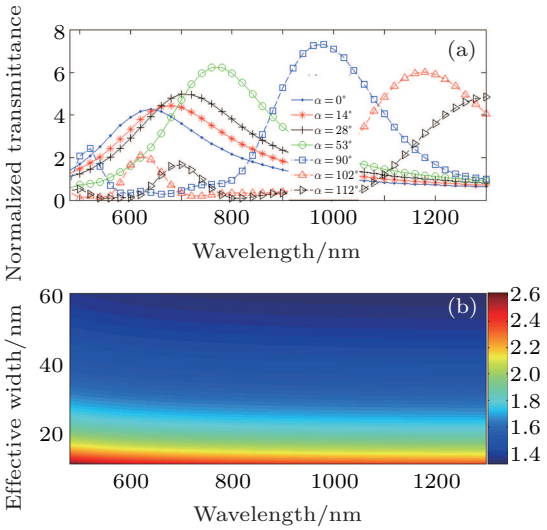


Fig. 2. (color online) (a) Transmission spectra of V-shaped nanoslit at different values of apex angle α, W_1, W_2, and H are taken as 30 nm, 30 nm, and 160 nm, respectively. (b) Variation of the real part of SPP mode ($\text{Re}(n_{\text{eff}})$) in oblique slit with the effective width of oblique slit ($W_{1(2)}\cos(\alpha/2)$) and the wavelength of SPP mode.

with the decrease of effective width (wavelength). The increase of α gives rise to the decrease of effective width, and the decrease of effective width further causes the increase of $\mathrm{Re}(n_{\mathrm{eff}})$. Thus, the increase of α leads to the increase of resonance wavelength according to the above F–P resonance formula. In addition, the increase of α also causes the increase of L [$\simeq H/\cos(\alpha/2)$]. Based on the above two factors, the resonance wavelength $\lambda_{\mathrm{res}N}$ of the V-shaped slit increases with the increase of α.

The change of transmission peak value in Fig. 2(a) seems to indicate that the enhanced transmission can be boosted up by using an optimum choice of the apex angle α. This phenomenon can be understood by a concrete picture in which the incident wave drives free electrons on the slit walls.[5,28] In order to elucidate such an issue, we schematically show the charge distribution and incident beam in Fig. 3. For the case of a vertical slit ($\alpha = 0°$, Fig. 3(a), the positive and negative charges, driven by the incident electric field, are accumulated at the left and right corners of the two ends of the slit, respectively. Thus two dipoles are formed at the entrance and exit of the slit. The dipoles at the entrance and exit oscillate with the incident wave, and then emit photons, giving rise to scattering and transmission, respectively. When α increases [$0° < \alpha < 180° - 2\tan^{-1}(H/W_{1(2)})$, Fig. 3(b)], four quasi-dipoles (the asymmetry of the left and right entrance/exit) are formed due to the introduction of the tapered metal bar in the slit, two of them are located at the two entrances of the V-shaped slit, the other two quasi-dipoles are positioned at the exit of the slit (there are a few charges near the apex of the tapered metal bar). In such a situation, the overall walls on the left and right sides of the V-shaped slit are illuminated by the incident beam. The total force, which is absence for the vertical slit, exerted by the incident wave on all the free electrons on the wall AB may be written as $F^{\mathrm{tot}} = [eE_{\mathrm{in}}\sin(\alpha/2)][H/\cos(\alpha/2)]I$, where E_{in} is the electric field of incident light and I is the photon density incident on the wall AB.[5] I is proportional to $\sin(\alpha/2)$, so $F^{\mathrm{tot}} \propto eE_{\mathrm{in}}H\sin^2(\alpha/2)/\cos(\alpha/2)$. The appearance of F^{tot} causes the change in the numbers of oscillating charges at the two ends of the slit. Specifically speaking, the oscillating electrons on the left-side wall AB are driven by the total force, and they move toward the entrance direction, so the number of positive charges at the entrance of the V-shaped slit decreases. The situation for the right oblique slit is contrary, the total force F^{tot} drives the oscillating electrons away from the entrance of the right wall of the right oblique slit. Hence, less negative charges accumulate at the entrance of the right wall of the right oblique slit. According to the above expression, the total force F^{tot} increases when α increases from $0°$ to $180° - 2\tan^{-1}(H/W_{1(2)})$, so the oscillating charges at the entrance end decrease with the increase of α. Even though two quasi-dipoles are in phase on the incidence surface and there is interference between them, the decrease of charges results in the drop of dipole moments, and thus the scattering energy decreases, which is in favor of the improvement of light transmission. On the other hand, the total force also has negative effects on the increase of charges at the exit end. However, the electromagnetic interaction between the quasi-dipoles at the exit end is different from that at the entrance due to the difference in distance between them, and it may be of benefit to the slit transmission. In fact, it should be noted that the eventual transmission value is also influenced by the ohmic loss besides the scattering energy. For the V-shaped slit structure, the ohmic loss of gap plasmon modes in the oblique slits increases in comparison with that in the corresponding vertical slit due to the increase of the imaginary part of effective refractive index n_{eff}. The increase of ohmic loss has negative effects on the slit transmission, while the decrement of scattering energy is larger than the increment of ohmic loss as α is changed from $0°$ to $180° - 2\tan^{-1}(H/W_{1(2)})$. Therefore the transmission value at resonant wavelength for a V-shaped slit is larger than that for the vertical slit.

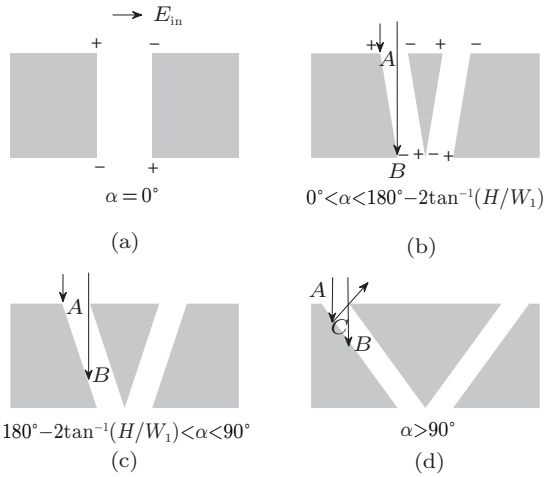


Fig. 3. Schematic representation of charge distribution and incident beam for different apex angle ranges: (a) $\alpha = 0°$, (b) $0° < \alpha < 180° - 2\tan^{-1}(H/W_1)$, (c) $180° - 2\tan^{-1}(H/W_1) < \alpha < 90°$, (d) $\alpha > 90°$. Here, E_{in} denotes the incident electric field.

If α further increases [$180° - 2\tan^{-1}(H/W_{1(2)}) < \alpha < 90°$, Fig. 3(c)], only part of the slit wall (AB) can be illuminated by the incident light, the total force F^{tot} is expressed by $[eE_{\mathrm{in}}\sin(\alpha/2)][W_{1(2)}/\sin(\alpha/2)]I$ ($= eE_{\mathrm{in}}W_{1(2)}I$), and $F^{\mathrm{tot}} \propto eE_{\mathrm{in}}W_{1(2)}\sin(\alpha/2)$. In such case, the total force increases continuously with the increase of α, and the changes of ohmic loss and scattering energy are similar to those in the range of $0° < \alpha < 180° - 2\tan^{-1}(H/W_{1(2)})$. Consequently, the transmission peak keeps growing with the increase of α. Once α exceeds $90°$ (Fig. 3(d)), the incident light on the slit wall AC is reflected back into the incidence space, which leads to the increase of the scattering energy. The scattering energy resulting from the reflection light increases with the increase of α. Even though the total force F^{tot} ($\propto eE_{\mathrm{in}}W_{1(2)}\sin(\alpha/2)$) suppresses the light scattering by the slit, eventually the scattering energy increases with the increase of α, since the scattering energy originating from the reflection in region of AC

becomes dominant in the total scattering energy. In the meantime, the ohmic loss presents a growth trend with the increase of α. Hence, the transmission peak drops.

The resonance wavelength of the V-shaped slit varies with the apex angle α, while the optical properties of the silver are not the same at different wavelengths. In order to further examine the effect of angle α on transmission value, we considered the case of modifying the film thickness H for each considered angle α such that the wavelength of transmission peak is fixed at 980 nm (Fig. 4(a)). It is clear that the optimum angle α with respect to the optimizing transmission value is about 90°. Also, in this case of fixed resonance wavelength, all apex angles smaller than 112° result in higher peak transmissions compared with the vertical slit (i.e., $\alpha = 0°$). The simulated results (not shown here) also show that there is almost the same ohmic loss for all film thicknesses, while the scattering energy approaches to its minimum at $\alpha \simeq 90°$, confirming the reasonableness of the above analysis. Both the optimum angles α in Figs. 2 and 4(a) are about 90°. Could we conclude that the optimum angles are 90° for other cases? The answer is no, since the total force is related to $W_{1(2)}$ apart from the angle α. Figure 4(b) shows the dependence of peak transmission on the angle α at different values of $W_{1(2)}$ (with fixed H). It is obvious that there are similar lineshapes for different $W_{1(2)}$, but with different optimum angle α. The optimum angles α in the cases of $W_{1(2)} = 20$ nm, 30 nm, and 60 nm are about 60°, 90°, and 96°, respectively. Such difference may be explained as follows. The total force F^{tot} is proportional to $W_{1(2)}$ (in the case of $\alpha > 180° - 2\tan^{-1} H/W_{1(2)}$), so larger $W_{1(2)}$ gives rise to larger F^{tot}. Meanwhile, the larger F^{tot} can experience more ohmic loss, and more ohmic loss is associated with larger α for the same H. Therefore, larger (smaller) $W_{1(2)}$ corresponds to larger (smaller) optimum angle α.

Next, we study the influence of symmetry breaking of the V-shaped slit on the transmission characteristics. Figure 5(a) illustrates the spectra of the V-shaped slit at different widths of $W_{1(2)}$ with fixed $W_1 + W_2 = 60$ nm. In the case of $W_1 = W_2 = 30$ nm, the V-shaped slit is a left–right-symmetric structure, there is a resonance peak at 760 nm in the transmission spectrum. When W_1 is changed to 25 nm, the left–right symmetry of the V-shaped slit is broken, the transmission peak is divided into two peaks located at 700 and 840 nm, respectively. With the further decrease of W_1, the asymmetry degree of the V-shaped slit increases, the long wavelength peak is redshifted, and its intensity is quickly decreased. Meanwhile, the change of the short wavelength peak in position and amplitude is rather small. To get more insight about such phenomena, we calculated the time-averaged density distributions of electric field

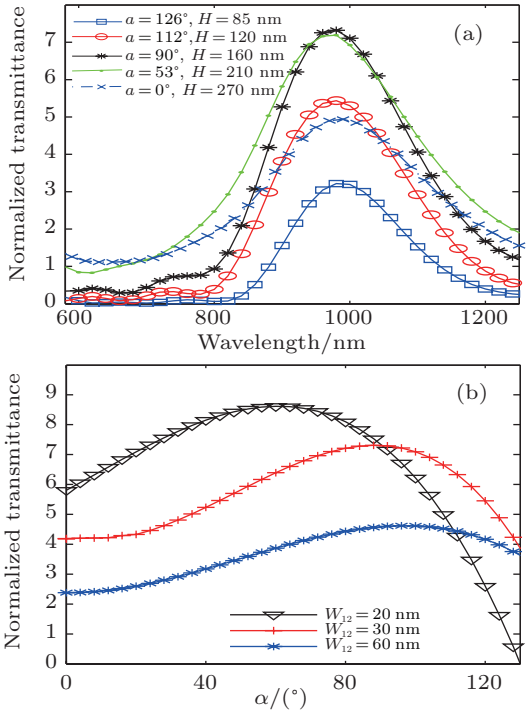


Fig. 4. (color online) (a) Transmission spectra for selected angles α with H adjusted to give a fixed peak transmission wavelength of 980 nm. (b) Peak transmission vs. angle α in the case of fixed H (= 160 nm).

$|E|$, as shown in Figs. 5(b)–5(d). Figures 5(b)–5(d) correspond to the resonance peaks at 760 nm ($W_1 = W_2 = 30$ nm), 700 nm ($W_1 = 20$ nm, $W_2 = 40$ nm) and 900 nm ($W_1 = 20$ nm, $W_2 = 40$ nm) in Fig. 5(a), respectively. At the resonance wavelength of a symmetric V-shaped slit structure (Fig. 5(b)), the fundamental resonant modes inside the left and right slits, which is characterized by an intensity minimum in the middle of the slit channel, are symmetrically excited. For the short wavelength peak at 700 nm in an asymmetric V-shaped slit (Fig. 5(c)), the electric field in the right slit is much more intense than that in the left slit, suggesting that only the right slit is resonant. The light transmission mainly comes from the right slit, so the transmission value is smaller than that of peak at 760 nm. With respective to the long wavelength peak at 900 nm (Fig. 5(d)), the field distribution is different from that in Fig. 5(c), only the fundamental resonant mode inside the left slit is effectively excited. The above phenomena can be explained as follows. In the structure of the left–right symmetric V-shaped slit, the right and left slits have the same resonance condition, so only one resonance peak appears in the transmission spectrum. Once the left-right symmetry is broken, the right and left slits have different resonance conditions, and the small (large) slit has a long (short) resonance wavelength due to large (small) $\text{Re}(n_{\text{eff}})$. Thus the resonance peak in the symmetric structure is split into two resonance peaks. The decease of W_1 causes the decrease (increase) of the effective width of the left (right) oblique slit, and the decrease (increase) of effective width further gives rise to the increase (decrease) of $\text{Re}(n_{\text{eff}})$ (as shown in Fig. 2(b)). Hence, the resonance wavelength of left (right) oblique slit increases (decreases) with

the decrease of W_1 according to the F–P resonance formula. $\mathrm{Re}(n_{\mathrm{eff}})$ in the small slit is more sensitive than that in the large slit to the change of slit width, so the long wavelength peak corresponding to the small slit (i.e., left oblique slit) exhibits a significant redshift, while the short wavelength peak corresponding to the large slit (i.e., right oblique slit) has a slight blueshift. Besides the above phenomena, we also note that the electric fields near the ends of the slit are over 15 times that of the incident light. Such large local electric field makes the V-shaped slit structure promising for a wide range of practical applications, e.g. within surface-enhanced spectroscopies. In this paper, we do not discuss the substrate effect. If a substrate is present underneath the V-shaped slit, the transmission peaks exhibit a redshift in comparison with the case without a substrate, and similar phenomena mentioned above can also be observed.

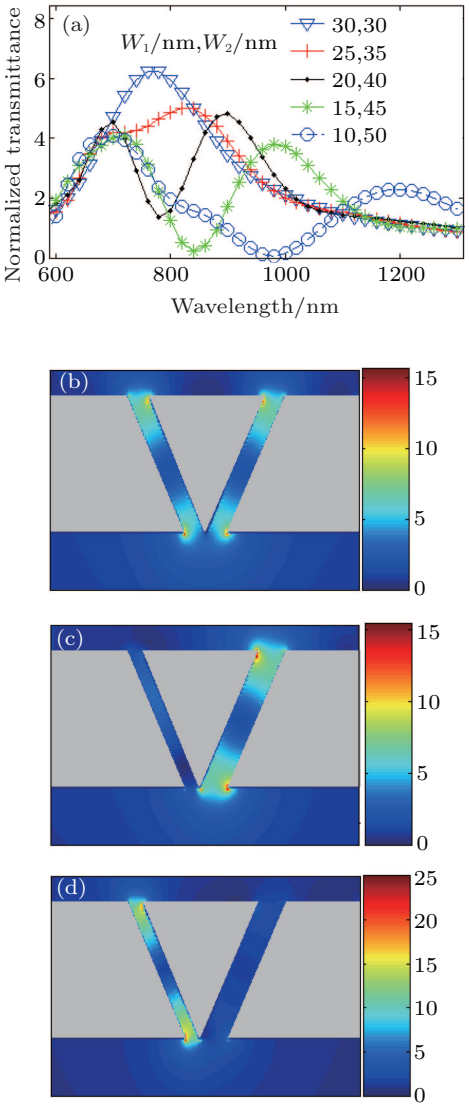


Fig. 5. (color online) (a) Transmission spectra of V-shaped nanoslit at different values of $W_{1,2}$ with fixed $W_1 + W_2 = 60$ nm, H and α are taken as 160 nm and 53°, respectively. Panels (b)–(d) correspond to the distributions of electric field $|E|$ for transmission peaks at 760 nm ($W_1 = W_2 = 30$ nm), 700 nm ($W_1 = 20$ nm, $W_2 = 40$ nm) and 900 nm ($W_1 = 20$ nm, $W_2 = 40$ nm), respectively. The incident plane wave with a unitary electric field is incident normally from the top.

4. Conclusion

In summary, we have investigated the transmission properties of a metallic V-shaped slit by using the 2D-FDTD method. It is found that the maximum transmission at resonance increases significantly by 71.5% in comparison with that of the vertical slit structure. The transmission spectrum is very sensitive to the apex angle of the V-shaped slit, and the slit width has an impact on the optimum apex angle. Such phenomena can be explained well by a concrete picture in which the incident wave drives free electrons on the conducting surfaces. Moreover, we simply discussed the effect of left–right asymmetry of the V-shaped slit on transmission spectrum. The symmetry breaking leads to the splitting of the transmission peak, and the transmission peak can be adjusted by the asymmetry degree of the V-shaped slit. We hope that our findings will be used to design the plasmonic devices based on metallic slit nanostructures.

References

[1] Ebbesen T W, Lezec H J, Ghaemi H F, Thio T and Wolff P A 1998 *Nature* **391** 667
[2] Porto J A, García-Vidal F J and Pendry J B 1999 *Phys. Rev. Lett.* **83** 2845
[3] Liu H and Lalanne P 2008 *Nature* **452** 728
[4] Xu H Q, Fu S L, Xie S X, Li H J and Zhou X 2010 *Chin. Phys. B* **19** 077803
[5] Huang X R, Peng R W and Fan R H 2010 *Phys. Rev. Lett.* **105** 243901
[6] Wang X D, Ye Y H, Ma J and Jiang M P 2010 *Chin. Phys. Lett.* **27** 094101
[7] Gorkunov M, Podivilov E and Sturman B 2011 *Phys. Rev. B* **83** 035414
[8] Bao Y J, Peng R W, Shu D J, Wang M, Lu X, Shao J, Lu W and Ming N B 2008 *Phys. Rev. Lett.* **101** 087401
[9] Li J, Iu H, Wan J T K and Ong H C 2009 *Appl. Phys. Lett.* **94** 033101
[10] Hua Y L, Fu J X, Li J Y, Li Z Y and Yang H F 2010 *Chin. Phys. B* **19** 047309
[11] Braun J, Gompf B, Weiss T, Giessen H, Dressel M and Hübner U 2011 *Phys. Rev. B* **84** 155419
[12] Anttu N, Guan Z Q, Håkanson U, Xu H X and Xu H Q 2012 *Appl. Phys. Lett.* **100** 091111
[13] Li G, Jin Z, Xue X, Lin X, Ma G, Hu S and Dai N 2012 *Appl. Phys. Lett.* **100** 191115
[14] Fan R H, Peng R W, Huang X R, Li J, Liu Y, Hu Q, Wang M and Zhang X 2012 *Adv. Mater.* **24** 1980
[15] Yang F and Sambles J R 2002 *Phys. Rev. Lett.* **89** 063901
[16] Takakura Y 2001 *Phys. Rev. Lett.* **86** 5601
[17] Wei F F, Wang H Y and Zhou Y S 2013 *Chin. Phys. B* **22** 024201
[18] Gan Q, Guo B, Song G, Chen L, Fu Z, Ding Y J and Bartoli F J 2007 *Appl. Phys. Lett.* **90** 161130
[19] López-Tejeira F, Rodrigo S G, Martín-Moreno L, García-Vidal F J, Devaux E, Ebbesen T W, Krenn J R, Radko I P, Bozhevolnyi S I, González M U, Weeber J C and Dereux A 2007 *Nat. Phys.* **3** 324
[20] García-Vidal F J, Lezec H J, Ebbesen T W and Martín-Moreno L 2003 *Phys. Rev. Lett.* **90** 213901
[21] Wang L, Cao J X, Liu L, Lv Y and Zheng S J 2008 *Appl. Phys. Lett.* **92** 241113
[22] Li Z, Caglayan H, Colak E and Ozbay E 2008 *Appl. Phys. Lett.* **92** 011128
[23] Wang C M, Huang H I, Chao C C, Chang J Y and Sheng Y 2007 *Opt. Express* **15** 3496
[24] Cui Y and He S 2009 *Opt. Lett.* **34** 16
[25] Min Q and Gordon R 2008 *Opt. Express* **16** 9708
[26] Sødergaard T, Bozhevolnyi S I, Novikov S M, Beermann J, Devaux E and Ebbesen T W 2010 *Nano Lett.* **10** 3123
[27] Sødergaard T, Bozhevolnyi S I, Beermann J, Novikov S M, Devaux E and Ebbesen T W 2012 *J. Opt. Soc. Am. B* **29** 130

[28] Huang X R, Peng R W, Wang Z, Gao F and Jiang S S 2007 *Phys. Rev. A* **76** 035802
[29] Baida F I and Van Labeke D 2003 *Phys. Rev. B* **67** 155314
[30] Yee K S 1966 *IEEE Trans. Antennas Propagat.* **14** 302
[31] Gray S K and Kupka T 2003 *Phys. Rev. B* **68** 045415
[32] Roden J A and Gedney S D 2000 *Microwave Opt. Technol. Lett.* **27** 334
[33] Hibbins A P, Lockyear M J and Sambles J R 2006 *J. Appl. Phys.* **99** 124903
[34] Wang B and Wang G P 2004 *Appl. Phys. Lett.* **85** 3599